73rd International Astronautical Congress (IAC), Paris, France, 18-22 September 2022.

IAC-22,B4,4,x67531

Monitoring and Early Detection of Wildfires Using Multiple-payload Fractionated Spacecraft

M. Amin Alandihallaj[a], M. Reza Emami[b]*

[a] *Institute for Aerospace Studies, University of Toronto, 4925 Dufferin Street, Toronto, Ontario M3H 5T6, Canada.*, amin.hallaj@alum.sharif.edu
[b] *Institute for Aerospace Studies, University of Toronto, 4925 Dufferin Street, Toronto, Ontario M3H 5T6, Canada.*, emami@utias.utoronto.ca
* Corresponding Author

Abstract

The paper discusses the deployment of multiple-payload fractionated spacecraft as a surveillance system for autonomously monitoring and detecting wildfires at early stages in any area on the Earth's surface. The fractionated system, consisting of 12 operational CubeSats, four reserved CubeSats, and one Mothership, acquires images in 13 spectral bands within the visible, near infrared, and short-wave infrared regions with high spatial resolutions. A dynamic fire-hazard index is introduced, based on geographic coordinates, environmental parameters, and weather conditions, to prioritize the areas for the probability of wildfires. Then, a convolutional neural network is designed to identify potentially hazardous areas and detect the early stages of wildfire spots. The detection method is based on the processed images and geographic locations as well as measurements of thermal anomalies, smoke, and unusual variations of regional atmospheric conditions. The effectiveness of the surveillance system is examined through several case studies using numerical simulations.

Keywords: Fire detection; Fractionated spacecraft; CubeSat; Convolutional neural network

Nomenclature

L_f	Dimensionless friction of the live vegetation
TN_f	Dimensionless friction of the fuel moisture
$H(p,q)$	Cross entropy of the distribution q relative to a distribution p

Acronyms/Abbreviations

BUI	Build Up Index
CNN	Convolutional Neural Network
COTS	Commercial off-the-shelf
DC	Drought Code
DFHI	Daily Fire Hazard Index
DL	Deep Learning
DMC	Duff Moisture Code
FFMC	Fine Fuel Moisture Code
FHI	Fire Hazard Index
FWI	Fire Weather Index
GSD	Ground Sampling Distance
ISI	Initial Spread Index
JRC	Joint Research Centre
MS	Multispectral
NN	Neural Network
ReLU	Rectified Linear Unit
SWIR	Short Wavelength Infrared
TRL	Technology Readiness Level
U	Unit
VNIR	Visible and Near Infrared
YOLO	You Only Look Once

1. Introduction

Forest fires have notable contributions to global warming by emitting a significant amount greenhouse gas. In addition, they can adversely affect human lives, ecosystem functionality and natural resources. The risk, duration and severity of forest fires are dramatically increasing due to climate change and human behavior, to the extent where the European Commission's Joint Research Centre (JRC) reports that a total area of about 500,000 hectares was burnt during 2021 in Europe region alone, which was 50% more than the average burnt-out area during 2008-2020 [1]. Therefore, a rapid and highly effective fire detection system is essential to reducing losses.

Traditionally, forest fires are detected by ground-based observations from fire lookout towers and/or heat, smoke, flame, and gas sensors implemented in specific locations inside the forests [2]. However, the relatively small range of such sensors, as well as human errors, cause limitations for early fire detection. Consequently, satellite-based early fire detection has been considered as a viable alternative. Further, recent developments in remote sensing, image processing, and machine learning, technologies have made spaceborne systems as an effective real-time tool for detecting forest fires.

The physical properties of flame and smoke can be measured by virtue of their apparent characteristics, such as color and texture, using optical sensors or RGB cameras onboard satellites. The main drawback of the color-based fire detection methods is their low accuracy [3]. Although the accuracy can be improved by combining data from optical and infrared cameras, the color-based methods have limited capacity in early fire detection in a complex area. In contrast, deep learning

(DL) methods can automatically extract and learn complex features, thus can be utilized for detecting the fire accurately in the early stages in a wide area [4]. Employing DL methods for forest fire detection has become an attractive research topic during the past decade. For example, a convolutional neural network (CNN)-based fire forest detection algorithm is developed in [5], consisting of five convolutional layers and three fully connected layers, which can detect the dynamic motion of the smoke. Similarly, CNN structures are proposed in [6] and [7] for fire and smoke detection. A two-layer fully connected neural network is utilized in [8] as an image classifier for detecting the fire. Forest fire detection using the surveillance videos is studied in [9] and [10], employing a fine-tuned CNN and optimized You-Only-Look-Once (YOLO) models, respectively. Moreover, a nine-layer CNN combined with a leaky rectified linear unit (ReLU) activation function is employed for fire detection [11]. A review of different approaches for forest fire detection can be found in [3].

Despite the capabilities of fire detection satellites, not all the fire spots in a vast area (larger than the satellite swath width) can be inspected simultaneously, due to the limitations of the imaging aperture. Thus, a potential fire out of the swath width may not be detected in the early stages. Although satellites can generally perform attitude maneuvers to change the access area, the slew rate of a large monolithic satellite with large optical sensors is limited. Consequently, some potential fire spots can remain undiscovered using a monolithic satellite.

One solution to monitoring all the potential fire spots in a vast area is to employ several separate imaging modules onboard multiple satellites in different orbits. A multiple-payload fractionated Earth observation system is introduced in [12, 13], which consists of twelve active and four reserved 8-unit CubeSats operating alongside a Mothership. The CubeSats are individually responsible for taking images, while the Mothership controls the mission, constructs wide-range images, and transmits data to Earth. Such a system makes it possible to monitor several potential fire spots simultaneously. Figure 1 illustrates the ability to monitor several fire spots simultaneously using a monolithic satellite versus distributed imagery.

This paper aims to study the effectiveness of enabling the multiple-payload fractionated Earth observation system as a surveillance system for monitoring and detecting wildfires in their early stages compared to an equivalent monolithic fire detection satellite. For this purpose, a brief overview of the multiple-payload fractionated Earth observation system is introduced in Section 2. Section 3 explains the methodology of fire detection process. Section 4 details the employed dynamic fire-hazard index for prioritizing the fire risk in different districts. Section 5 discusses the convolutional neural network for identifying the potentially hazardous

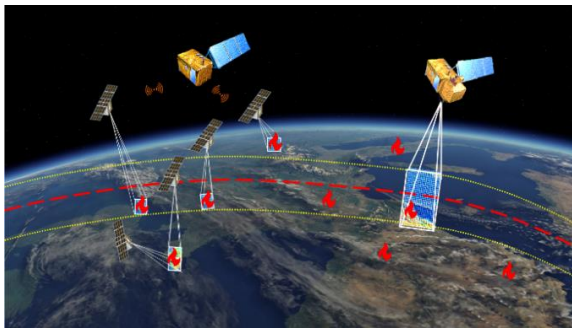

Figure 1. An illustrative comparison of the monolithic satellite and the fractionated spacecraft system regarding monitoring several fire spots.

areas and detecting the early stages of wildfire spots. Then, the effectiveness of the system is investigated through some numerical simulations presented in Section 6. Finally, some concluding remarks are made in Section 7.

2. Overview of multiple-payload fractionated spacecraft

The Multiple-payload Fractionated Earth Observation System consists of twelve active and four reserved homogeneous eight-unit (8U) CubeSats operating with a single Mothership, as illustrated in Figure 2. Each CubeSat, designed using available Commercial off-the-shelf (COTS) components with technology readiness level (TRL) of 8-9, carries two payload, namely, one multispectral (MS) camera from Simera-Sense [14] and one short wavelength infrared (SWIR) camera from Sensors Unlimited [15], to provide data in visible (VIS), near-infrared (NIR), and SWIR spectral bands. The MS camera provides a ground sampling distance (GSD) of 7.5 m and a swath-width of 30.7 km, and the SWIR camera is capable of achieving a GSD better than 20 m and a swath-width of 25.4 km at 786 km orbit altitude. Each CubeSat has a 3-axis pointing control system, consisting of four reaction wheels mounted in a tetrahedral configuration combined with one three-axis magnetorquer, to precisely track the imaging region designated by the Mothership.

The Mothership serves as an interface between the

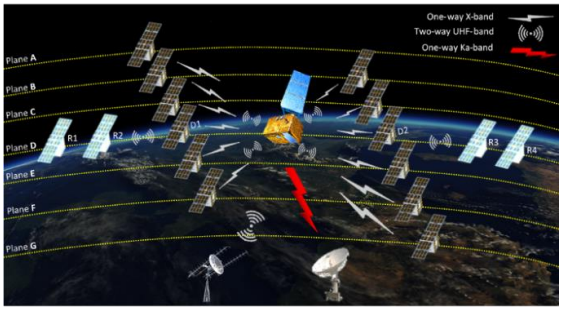

Figure 2. An illustration of the overall configuration of Multiple-Payload Fractionated Earth Observation System.

imagery system (CubeSats) and the ground station. It also manages the CubeSats, through computing the attitude reference, allocating the imaging tasks, determining the CubeSats orbits, predicting the collisions, and calculating the orbital maneuver for the CubeSats, by employing a two-way UHF-band (430-440 MHz) communication channel. Moreover, the Mothership processes received raw images from the CubeSats throughout a one-way X-band (8.025-8.400 GHz) channel for transmitting to the ground station in the Ka-band.

3. Methodology

The Mothership identifies the CubeSats tasks, and the CubeSats serve as a distributed imagery system. First, the Mothership receives the environmental information from the ground station(s), including temperature, wind, humidity, etc., to generate the fire-hazard index map, which shows the probability of fire occurrence in each area. Next, potential fire spots are identified by the Mothership and then allocated to the CubeSats for taking images from. After receiving images from the CubeSats, the Mothership employs a CNN to determine if fires have occurred in a specific location. If the fire occurs, the location and the images of the fire are transmitted to the ground station. Then, the rest of identified potential fire spots are reallocated to the CubeSats. The schematic diagram of this process is shown in Figure 3. Detailed information regarding the task reallocation technique can be found in [13].

4. Dynamic fire-hazard index

The probability of fire occurrence in a specific location is usually calculated using a fire index, which can be a function of environmental variables such as land cover, altitude, land slope, fuel type, etc. The required information for the fire hazard calculation is traditionally employed as a static layer, which may neglect significant effects on the fire risk related to the seasonal and daily changes [16].

The fire weather index (FWI) system is one of the substantial tools for predicting forest fires, whose purpose is to determine the effects of the weather on forest fires. The FWI utilizes the historical daily values of the air temperature, relative humidity, wind speed, and rainfall quantity provided by weather stations. The FWI consists of three sub-indexes, as follows [17]:

- fine fuel moisture code (FFMC), which represents the moisture content of fine fuels;
- duff moisture code (DMC), which gives the moisture content of loosely compacted, decomposing organic matter; and
- drought code (DC), which denotes a deep layer of compact organic matter.

The three primary sub-indexes in conjunction with the wind are used to produce the two intermediate sub-indexes, initial spread index (ISI) and build up index

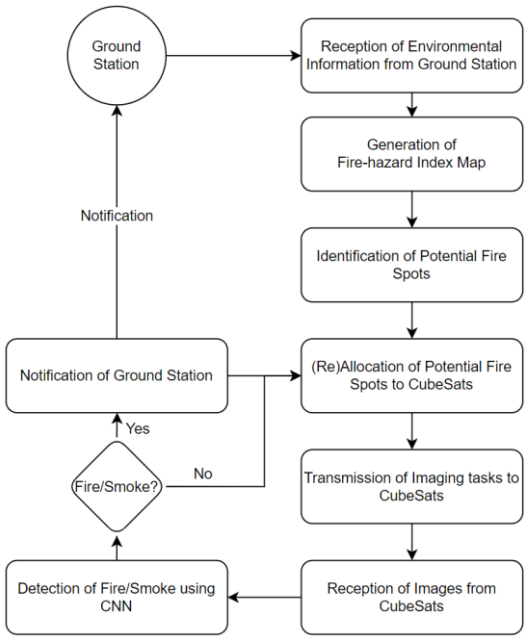

Figure 3. The schematic diagram of the fire detection process.

(BUI). The final FWI is then formed by combining the intermediate sub-indexes, representing the intensity of the spreading fire due to weather. More detailed information regarding the FWI system can be found in [17].

The main drawback of the FWI is that the index is only based on meteorological information. However, other factors such as topography information, vegetation cover, and history may affect the fire ignition and the spread speed [18]. It is shown in [19] that the fire risk can be more accurately predicted in woodland by taking the long-term vegetation dynamics into consideration. Thus, the FWI should be modified according to the specific information for each area. For this purpose, the FWI can be combined with daily fire-hazard index (DFHI) [20] for employing the satellite data, fuel maps, and historical fire records of a certain area to predict the fire-hazard probability more accurately. The DFHI can be calculated using the dimensionless friction of the live vegetation, L_f, and the dimensionless friction of the fuel moisture, TN_f, with respect to the values registered in the area of interest during the five last year, as follows [20]:

$$\mathrm{DFHI} = (1 - L_f)(1 - TN_f) \quad (1)$$

Detailed information about calculating L_f and TN_f can be found in [20].

Since both FWI and DFHI hold values in the [0, 1] interval, the final fire-hazard index (FHI) can then be calculated as the average of FWI and DFHI that can be translated to a categorical probability as described in . Moreover, the diagram of calculating FHI is shown in Figure 4.

Table 1 The classification of the fire probability based on FHI.

Fire-hazard Index	Fire Probability Class
0.00-0.25	No probability
0.25-0.50	Low probability
0.50-0.75	Medium probability
0.75-1.00	High probability

5. CNN-based fire detection

The forest fire detection problem can be transferred into a classification problem, where a CNN is utilized to determine the fire and/or smoke on satellite images. The general information about utilizing CNN for machine learning, including the training and test processes, is detailed in [21]. The employed CNN is formed of three convolutional models (with the convolution kernel size of 2, 3, and 4) and a fully connected layer. Each convolutional model has two convolutional layers with a leaky rectified linear unit (ReLU) activation function and a maximum pooling layer. After passing through the fully connected layers, the final layer employs the SoftMax activation function, which is used to get probabilities of the input being in a particular class of fire/smoke/no-event. Finally, the cross-entropy is chosen as the loss function, which can be defined as follows [22]:

$$H(p,q) = \sum_{x} p(x) \log q(x) \qquad (2)$$

The general structure of the employed CNN can be seen in Figure 5, where convolutional layers are indicated by blue color, maximum pooling layers are designated in white color, and fully connected layers are illustrated in red.

6. Numerical simulation

In this section, two case studies are presented to investigate the effectiveness of the proposed fire-hazard index and the performance of fractionated spacecraft in monitoring multiple potential fire spots.

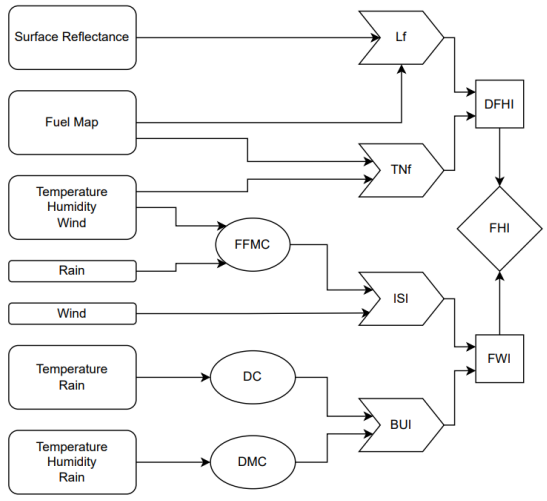

Figure 5. the diagram of calculating FHI.

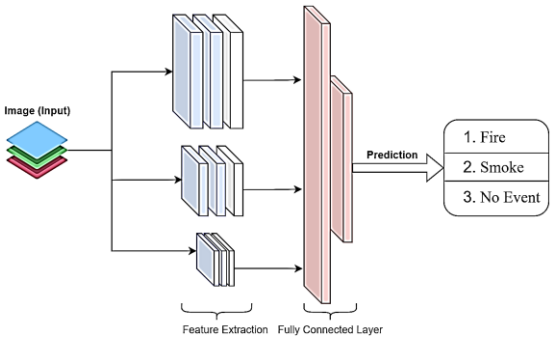

Figure 4. The general structure of the employed CNN.

For studying the effectiveness of the fire-hazard index the forests southeast of the Caspian Sea are selected, which is indicated by red borders in Figure 6. The geographical coordinates of the area are within [54°43′ 56°01′] E and [36°44′ 37°29′] N, which is approximately 116 km long and 30 km wide. Over 14550 hectares of the area were burnt during October and November 2010 [23]. All affecting data on FHI for the study area during the mentioned period were obtained

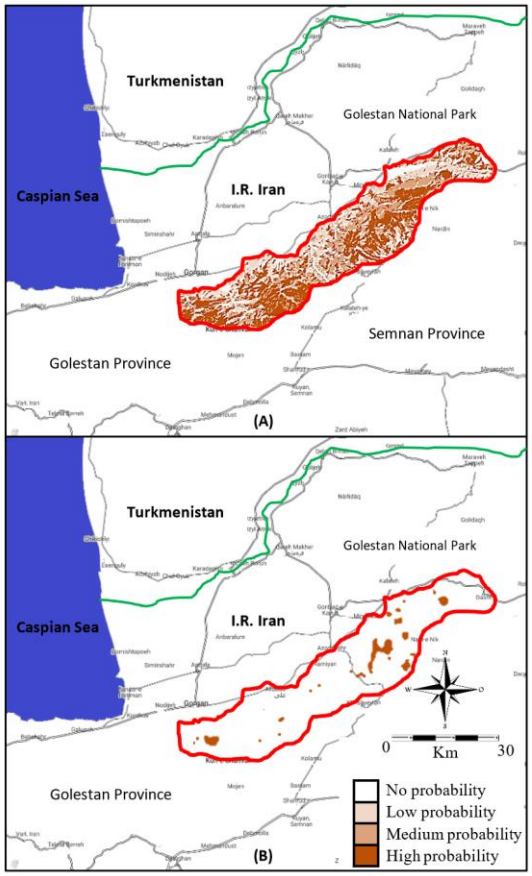

Figure 6. Probability of the forest fire over the study area: A) The fire probability class map according to FWI, B) Potential fire spots designated by FHI.

from the National Cartographic Center (NCC) of I.R. Iran and daily meteorological data from available synoptic-climatological stations in Golestan Province to generate the fire-hazard map.

Figure 6 compares the probability of the fire over the study area based on FWI and FHI. It can be seen from the figure that using FWI, 28% of the study area is identified as high probability class, 33% as medium probability class, 31% as low probability class, and 8% as no fire probability class. However, the area of high fire probability estimated by FHI is only 5%, which practically contains all the actual fire spots that should indeed be flagged by the surveillance system.

In order to study the fire detection performance of fractionated system and compare it with that of a monolithic satellite, fire scenarios in two regions of the Europe are considered, i.e., a small area (410km × 400km, indicated by blue borders in Figure 7) and a large area (1200km × 800km, indicated by red borders in Figure 7). In each area, several fire spots are put randomly in the area (the *x* and *y* coordinates of each random point follow a uniform distribution). The performance of the fractionated system for a certain number of fire spots in each area is compared to that of its Sentinel-2 counterpart through a Monte-Carlo simulation (5000 runs for each number of fire spots in each area).

The performance criterion, as a success ratio, is the number of detected fire spots to the total number of fire spots. In order to detect a fire spot, each point that is identified as a potential fire spot (using FHI map) must be observed for 10 seconds to compute the CNN, during a satellite's single pass of 10 minutes for surveilling the area (in one orbit). According to the agility requirement for Sentinel-2 [24], the maximum slew rate is 0.5 degrees per second. It should be noted that when a potential fire spot is being observed and other potential spots are in the satellite's field of view, all of these spots are checked simultaneously.

Figure 8 illustrates the success ratio of Sentinel-2 and fractionated spacecraft in the small area. It can be seen that using Sentinel-2 guarantees a success ratio of 100%, because the 290 km swath-width of Sentinel-2 [25]

Figure 9. The study area for the fire searching scenario.

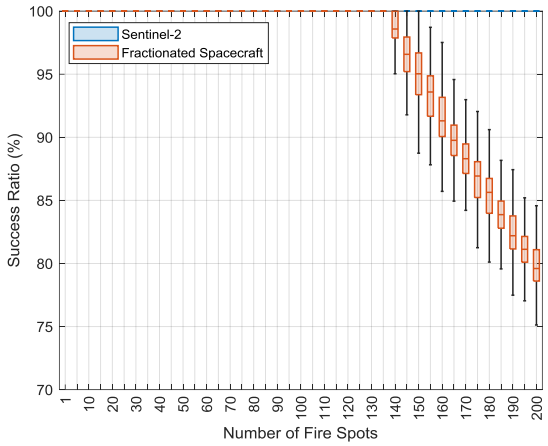

Figure 8. The effect of number of potential fire spots on the success ratio in the small area.

covers several fire spots at each imaging shot in the small area. However, since the maneuvering time increases with the number of fire spots, the performance of the fractionated spacecraft degrades when the number of fire spots exceeds 140.

The success ratios of Sentinel-2 and fragmented spacecraft in the large area are compared in Figure 9. It can be seen from the figure that although the performance of both systems degrades with the increase in the number of fire spots, fractionated spacecraft has outperformed Sentinel-2. The reason is that twelve fire spots are investigated simultaneously by the CubeSats of the fractionated system, whereas because of the long distances between fire spots (unlike the small area), only one of such spots may be investigated at any time using Sentinel-2. Thus, by increasing the number of spots to more than 10, the performance of Sentinel-2 degrades dramatically.

One can argue that Sentinel-2 would be able to cover the large area in multiple passes. However, it is essential to note that since the revisit time of a single operational

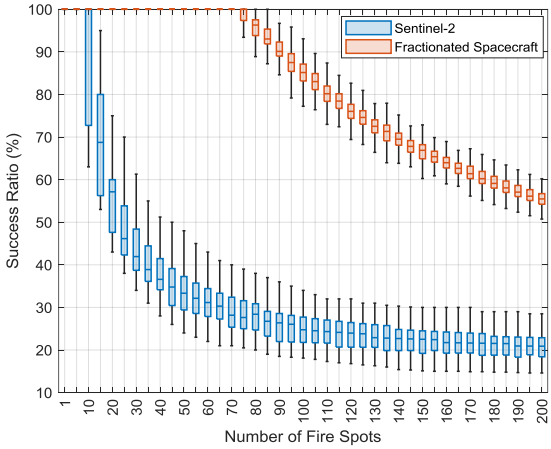

Figure 7. The effect of number of potential fire spots on the success ratio in the large area.

Sentinel-2 satellite is ten days [26], investigation of all fire spots in a large area may take a long time. Thus, wildfires may not be detected in their early stages.

7. Conclusion

The feasibility of employing multiple-payload fractionated spacecraft as a surveillance system for detecting wildfires at early stages was studied in this paper. A dynamic fire-hazard index was introduced for identifying potentially hazardous areas. The index is employed in conjunction with a neural network, consisting of three convolutional models and a fully connected layer, for detecting fire in the hazardous areas. The numerical simulations showed that combining the fire weather index with daily weather information, fuel maps, and historical fire records can estimate the fire hazard probability more accurately. Through a stochastic performance analysis, it was shown that the notion of fractionated spacecraft can be logistically viable for a fire detection surveillance system in a large area. The results revealed that although Sentinel-2, an operational monolithic satellite, can be more effective than the fractionated spacecraft in detecting fire in a small area, wildfires in a large area may not be detected in the early stages using a monolithic satellite because of the long revisit time. In contrast, the fractionated spacecraft can detect more fire points in a shorter time than the monolithic satellite over a larger area.

References

[1] Joint Research Centre, "Forest Fire in Europe, Middle East, and North Africa 2021," JRC , Ispra (Italy), 2022.

[2] O. Kucuk, O. Topaloglu and A. Altunel, "Visibility analysis of fire lookout towers in the Boyabat State Forest Enterprise in Turkey," *Environ Monit Assess,* vol. 189, no. 329, 2017.

[3] P. Barmpoutis, P. Papaioannou, K. Dimitropoulos and N. Grammalidis, "A Review on Early Forest Fire Detection Systems Using Optical Remote Sensing," *Sensors,* vol. 20, no. 6442, 2020.

[4] J. Schmidhuber, "Deep learning in neural networks: An overview," *Neural Network,* vol. 61, p. 85–117, 2015.

[5] Y. Luo, L. Zhao, P. Liu and D. Huang, "Fire smoke detection algorithm based on motion characteristic and convolutional neural networks," *Multimedia Tools and Applications,* vol. 77, pp. 15075-15092, 2018.

[6] X. Wu, X. Lu and H. Leung, "An adaptive threshold deep learning method for fire and smoke detection," in *2017 IEEE International Conference on Systems, Man, and Cybernetics (SMC)*, Banff, AB, Canada, 2017.

[7] J. Sharma, O. Granmo, M. Goodwin and J. Fidje, "Deep convolutional neural networks for fire detection in images," in *International Conference on Engineering Applications of Neural Networks*, Athens, Greece, 2017.

[8] Q. Zhang, J. Xu, L. Xu and H. Guo, "Deep convolutional neural networks for forest fire detection," in *International Forum on Management, Education and Information Technology Application*, Paris, France, 2016.

[9] K. Muhammad, J. Ahmad, I. Mehmood, S. Rho and S. Baik, "Convolutional neural networks based fire detection in surveillance videos," *IEEE Access,* vol. 6, pp. 18174-18183, 2018.

[10] D. Shen, X. Chen, M. Nguyen and W. Yan, "Flame detection using deep learning," in *the 2018 4th International Conference on Control, Automation and Robotics (ICCAR)*, Auckland, New Zealand, 2018.

[11] S. Frizzi, R. Kaabi, M. Bouchouicha, J. Ginoux, E. Moreau and F. Fnaiech, "Convolutional neural network for video fire and smoke detection," in *the IECON 2016-42nd Annual Conference of the IEEE Industrial Electronics Society*, Florence, Italy, 2016.

[12] M. A. Alandihallaj and M. R. Emami, "Multiple-payload fractionated spacecraft for earth observation," *Acta Astronautica,* vol. 191, pp. 451-471, 2022.

[13] M. A. Alandihallaj and M. R. Emami, "Satellite replacement and task reallocation for multiple-payload fractionated Earth observation mission," *Acta Astronautica,* vol. 196, pp. 157-175, 2022.

[14] "MultiScape100 CIS," Simera Sense, [Online]. Available: https://simera-sense.com/products/multiscape100-cis. [Accessed 1 March 2021].

[15] "Mini-SWIR 1280JSX High Definition Camera," Sensors Unlimited,, [Online]. Available: http://www.sensorsinc.com/products/detail/mini-swir-jsx-snapshot-camera-60-fps. [Accessed 1 March 2021].

[16] Y. Michael, D. Helman, O. Glickman, D. Gabay, S. Brenner, I. M. Lensky, D. Helman, O. Glickman, G. David, S. Brenner and I. M. Lensky, "Forecasting fire risk with machine learning and dynamic information derived from satellite vegetation index time-series," *Science of The Total Environment,* vol. 764, no. 142844, 2021.

[17] C. Van Wagner, "Development and Structure of the Canadian Forest Fire Weather Index

System," Government of Canada, Canadian Forestry Service, Ottawa, ON, Canada, 1987.

[18] M. C. De Jong, M. J. Wooster, K. Kitchen, C. Manley, R. Gazzard and F. F. McCall, "Calibration and evaluation of the Canadian Forest Fire Weather Index (FWI) System for improved wildland fire danger rating in the United Kingdom," *Natural Hazards and Earth System Sciences,* vol. 16, no. 5, pp. 1217-1237, 2016.

[19] D. Helman, I. Lensky, N. Tessler and Y. Osem, "A Phenology-Based Method for Monitoring Woody and Herbaceous Vegetation in Mediterranean Forests from NDVI Time Series," *Remote Sensing,* vol. 7, pp. 12314-12335, 2017.

[20] G. Laneve, V. Pampanoni and R. Uddien Shaik, "The Daily Fire Hazard Index: A Fire Danger Rating Method for Mediterranean Areas," *Remote Sensing,* vol. 12, no. 2356, 2020.

[21] R. Venkatesan and L. Baoxin, Convolutional neural networks in visual computing: a concise guide, CRC Press, 2017.

[22] Y. Ho and S. Wookey, "The real-world-weight cross-entropy loss function: Modeling the costs of mislabeling," *IEEE Access,* vol. 8, pp. 4806-4813, 2019.

[23] O. Abdi, B. Kamkar, Z. Shirvani, J. Teixeira da Silva and M. Buchroithner, "Spatial-statistical analysis of factors determining forest fires: a case study from Golestan, Northeast Iran," *Geomatics, Natural Hazards and Risk,* vol. 9, no. 1, pp. 267-280, 2018.

[24] G. Wiedermann, W. Gockel, S. Winkler, J. Rieberm, B. Kraft and D. Reggio, "The SENTINEL-2 satellite attitude control system–challanges and solutions," in *9th International ESA Conference on Guidance, Navigation & Control Systems*, Oporto, Portugal, 2014.

[25] J. Transon, R. D'Andrimont, A. Maugnard and P. Defourny, "Survey of Hyperspectral Earth Observation Applications from Space in the Sentinel-2 Context," *Remote Sensing,* vol. 10, no. 2, 2018.

[26] M. Drusch, U. Del Bello, S. Carlier, O. Colin, V. Fernandez, F. Gascon, B. Hoersch, C. Isola, P. Laberinti, P. Martimort, A. Meygret, F. Spoto, O. Sy, F. Marchese and P. Bargellini, "Sentinel-2: ESA's Optical High-Resolution Mission for GMES Operational Services," *Remote Sensing of Environment,* vol. 120, pp. 25-36, 2012.